J Biomol NMR (2014) 60:67–71
DOI 10.1007/s10858-014-9852-0

NMR STRUCTURE NOTE

Structure of the membrane protein MerF, a bacterial mercury transporter, improved by the inclusion of chemical shift anisotropy constraints

Ye Tian · George J. Lu · Francesca M. Marassi · Stanley J. Opella

Received: 6 May 2014 / Accepted: 4 August 2014 / Published online: 8 August 2014

Biological context

Bacteria that survive in mercury-polluted environments contain an operon whose proteins constitute a mercury detoxification system (Barkay et al. 2003) that functions by importing highly toxic Hg(II) into the cytoplasm of the bacterial cell and enzymatically transforming it to its less toxic and volatile form Hg(0), which is passively eliminated. Initially, Hg(II) binds to the periplasmic protein MerP, which delivers it to a membrane protein transporter such as MerF. The membrane protein is responsible for transporting Hg(II) across the cell membrane and delivering it to MerA, the cytoplasmic mercuric reductase, a multi-domain enzyme that reduces Hg(II) to Hg(0). Understanding the molecular mechanism of mercury detoxification is important for both environmental and biomedical applications of components of the bacterial mercury detoxification system. Atomic resolution structures of MerP and MerA have been determined (Schiering et al. 1991; Steele and Opella 1997). Neither MerF nor any other mercury transport membrane proteins, e.g. MerT, MerC, from various isolates of bacterial mercury detoxification systems have been crystallized. Therefore, at present, NMR is the only viable approach to the structure determination of the membrane transport component of the detoxification system.

MerF (Wilson et al. 2000), with 81 residues and two transmembrane helices connected by a short, structured interhelical loop, is the smallest of the mercury transport membrane proteins. Notably, a pair of vicinal Cys residues that bind Hg(II) are associated with each transmembrane helix. Both Cys pairs are located on the cytoplasmic side of the protein, one pair in the middle of the N-terminal helix and the other near the C-terminal end of the second helix (Lu et al. 2013). They are in relatively close spatial proximity and one can envision a mechanism whereby Hg(II) ions are exchanged between the pairs of Cys residues. To avoid protein aggregation and extend the sample life for signal averaging, we mutated all four Cys residues to Ser residues. Direct spectroscopic comparisons show that the wild type and mutated forms of the protein have essentially the same structures.

Previously, we determined the structures of full-length MerF (Lu et al. 2013), and its N- and C- terminal truncated form, MerFt (Das et al. 2012) in phospholipid bilayers by rotationally aligned (RA) solid-state NMR. RA solid-state NMR combines elements of Oriented Sample (OS) solid-state NMR of stationary, aligned samples and magic angle spinning (MAS) solid-state NMR of unoriented proteoliposomes. Here, we utilize experimental results from both approaches to measure chemical shift anisotropy (CSA) restraints and improve the accuracy and precision of the structure of MerF in phospholipid bilayers. Several structures of membrane proteins, determined in phospholipid bilayers with OS NMR orientation restraints, have demonstrated the significant benefits of including ^{15}N CSA values as structural restraints (Ding et al. 2013; Murray et al. 2013; Opella 2013). Also CSA restraints measured

Electronic supplementary material The online version of this article (doi:10.1007/s10858-014-9852-0) contains supplementary material, which is available to authorized users.

Y. Tian · G. J. Lu · S. J. Opella (✉)
Department of Chemistry and Biochemistry, University of California San Diego, 9500 Gilman Drive, La Jolla, CA 92093-0307, USA
e-mail: sopella@ucsd.edu

Y. Tian · F. M. Marassi
Sanford-Burnham Medical Research Institute, 10901 North Torrey Pines Road, La Jolla, CA 92037, USA

from powder patterns of individual sites under MAS, were shown to improve the structural quality for a globular, crystalline protein (Wylie et al. 2011). Furthermore, we include additional NMR data that definitively show which of the terminal residues in the full-length protein are mobile in phospholipid bilayers.

Methods and results

Protein preparation

Preparation of MerF for NMR experiments has been described in detail (Lu et al. 2013). Briefly, full-length MerF was expressed and purified from *E. coli* with several different isotopic labeling schemes, including selective and uniform ^{15}N labeling for OS solid-state NMR and uniform ^{13}C and ^{15}N labeling for MAS solid-state NMR. For OS solid-state NMR studies, the protein was reconstituted into 1,2-dimyristoyl-sn-glycero-3-phosphocholine (DMPC) and 1,2-dihexanoyl-sn-glycero-3-phosphocholine (DHPC), at a DMPC/DHPC ratio of 3.2:1, to obtain magnetically aligned bicelle samples. For MAS solid-state NMR studies the protein was reconstituted in DMPC liposomes. In both cases, exhaustive dialysis was performed to remove any residual SDS used in reconstitution, and the pH was adjusted to 6.0. The "flipped" bicelle sample, with the bilayer normal parallel to the external magnetic field, was prepared by addition of $\sim$1.5 mM $YbCl_3$ to the preformed protein-containing bicelles.

NMR spectroscopy

OS solid-state NMR experiments were performed on a 700 MHz Bruker Avance spectrometer with a home-built ^{1}H/^{15}N double-resonance strip shield "low-E" probe. The sample temperature was maintained at 42 °C. The ^{15}N chemical shift frequencies were referenced to external solid ammonium sulfate at 26.8 ppm. The ^{1}H chemical shift frequencies were internally reference to $^{1}H_2O$ at 4.7 ppm. Two-dimensional separated local field (SLF) experiments were performed on unflipped bicelle samples, with the bilayer normals perpendicular to the field. Two-dimensional heteronuclear correlation (HETCOR) and three-dimensional HETCOR/SLF spectra were acquired to obtain OS solid-state NMR resonance assignments and measure CSA and dipolar coupling (DC) frequencies (Lu and Opella 2014).

In the MAS experiments, ^{13}C/^{13}C correlation was achieved with proton driven spin diffusion (PDSD) to qualitatively measure ^{13}C–^{13}C distances; mixing times of 50 and 200 ms were used, respectively, to extract short-range and long-range distance restraints. Three-dimensional HNCA (^{1}H–^{15}N DC/^{15}N CS/^{13}CA CS), HNCO (^{1}H–^{15}N DC/^{15}N CS/^{13}CO CS), and HCXCX (^{1}H–^{13}C DC/^{13}C CS/^{13}C CS) experiments were performed (Das

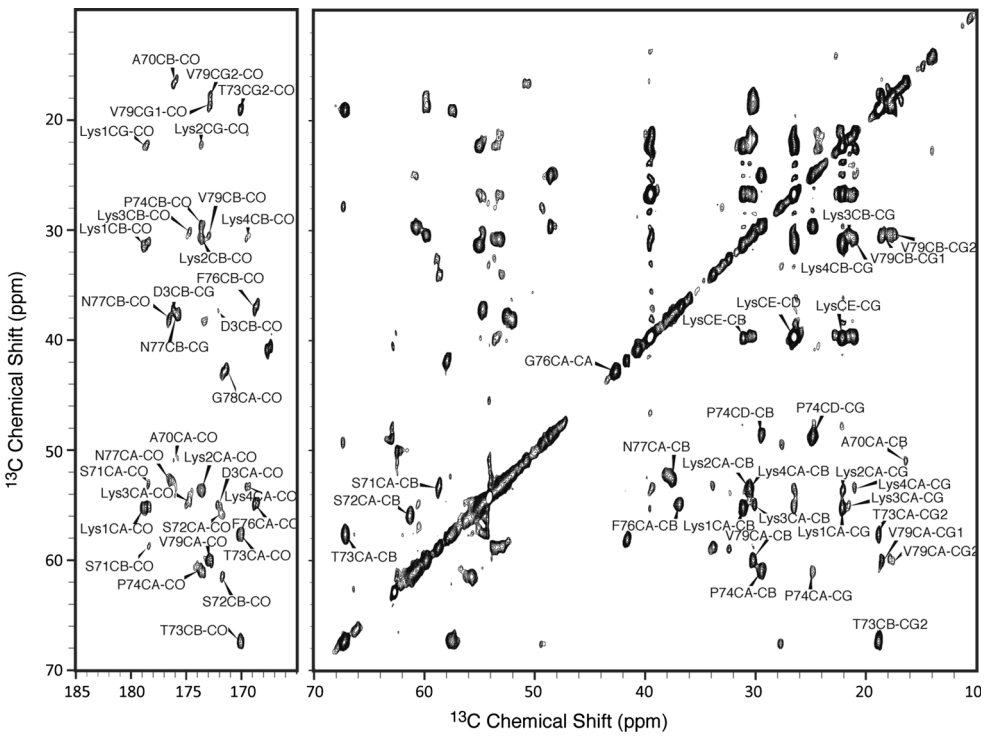

Fig. 1 Two-dimensional through-bond ^{13}C–^{13}C correlation spectrum with resonances assigned to mobile residues

et al. 2012). SPECIFIC-CP was utilized for magnetization transfer (Baldus et al. 1998). The $R18_1^7$ symmetry pulse sequence was employed for heteronuclear dipolar recoupling. MAS was performed at 11.111 kHz for the HNCA and HNCO experiments and at 13.889 kHz for HCXCX experiments. All of the MAS experiments were carried out at 25 °C. Two-dimensional through-bond correlation spectroscopy was used to identify the mobile residues undergoing isotropic motion where the INEPT pulse scheme selectively transfers polarization from ^{1}H to ^{13}C only for the mobile residues (Hardy et al. 2001). Details of the pulse sequence are shown in Fig. S1. The spectrum with assignments for the mobile terminal residues is shown in Fig. 1.

Structure calculations

Structure calculations were performed using a two-stage protocol (Das et al. 2012) designed to achieve atomic resolution three-dimensional structures of membrane proteins.

Three and nine residue fragments were initially generated on the Robetta server of Rosetta (Kim et al. 2004) based on the primary amino acid sequence of MerF. A total of 30,000 course-grained decoys were calculated on a local workstation, using the membrane protocol of Rosetta (Yarov-Yarovoy et al. 2006). All 30,000 decoys were refined against 50 experimental solid-state NMR NH DC restraints, in the Rosetta all-atom mode. After all-atom refinement, decoys were clustered using a cluster radius of 6 Å, for residue 5 through 73. This yielded a total of 45 clusters of which the most populated cluster (37.2 % population) contained 11,168 candidate decoys. The 1,000 lowest energy structures in this cluster were accepted and used to extract dihedral angle restraints. The lowest energy candidate was used as the initial structural model for further refinement by simulated annealing in Xplor-NIH (Schwieters et al. 2003) using all available experimental restraints (Table 1).

The Xplor-NIH refinement protocol was based on the internal variable module (Schwieters and Clore 2001) and comprised four stages: (1) torsion angle dynamics at high-temperature (3,000 K) for a period of 15 ps or 15,000 time steps, (2) torsion angle dynamics with simulated annealing, where the temperature is reduced from the initial high temperature value to 50 K in steps of 12.5 K, for a period of 0.2 ps or 1,000 time steps per temperature step, (3) 500 steps of Powell torsion angle minimization, and (4) 500 steps of Powell Cartesian minimization.

Experimental dihedral angle and distance restraints were applied with respective force constants of k_{CDIH} = 300 kcal mol^{-1} rad^{-2} and k_{dis} = 20 kcal mol^{-1} Å^{-2}. Experimental ^{1}H/^{15}N DC restraints were applied with a force constant set to 1 kcal mol^{-1} rad^{-2} in the high temperature stage, and ramped from 1 to 3 kcal mol^{-1} rad^{-2} for unsigned DC restraints, or 1–5 kcal mol^{-1} rad^{-2} for signed DC restraints during the annealing stage. Experimental ^{15}N CSA and ^{1}HA-^{13}CA DC restraints were applied with force constants of 0.1 kcal mol^{-1} rad^{-2} at high temperature and ramped from 0.1 to 0.5 kcal mol^{-1} rad^{-2} during annealing. The axial alignment parameter (Da) was initially set to 10.0 kHz and allowed to vary during the calculation. The rhombicity parameter (Rh) was fixed at 0.0 to reflect the uniaxial alignment of the samples used in the solid-state NMR experiments (Tian et al. 2012). The ^{15}N CSA restraints were implemented with generic ^{15}N tensors of $\delta_{11} = -42.3$ ppm, $\delta_{22} = -55.3$ ppm, $\delta_{33} = 97.7$ ppm, $\delta_{iso} = 119.3$ ppm, $\beta = 17°$, and $\gamma = 0°$ for all

Table 1 Experimental restraints and structural statistics

Number of NMR restraints	
[a]DC ^{1}H/^{15}N (signed/unsigned)	45/14
[a]DC ^{1}HA/^{13}CA	58
[b]DC ^{1}H/^{15}N (signed/unsigned)	50/14
[b]CSA ^{15}N	64
[c]Distances ^{13}C–^{13}C (long-range, $>i-i+4$)	1
[c]Distances ^{13}C–^{13}C (short-range, $<i-i+4$)	48
[d]Dihedral angles	148
Structure statistics	
Deviations from idealized geometry (RMSD and standard deviation)	
Bond lengths (Å)	0.005 ± 0.000
Bond angles (°)	1.060 ± 0.014
Impropers (°)	1.512 ± 0.060
Violations (RMSD and standard deviation)	
[a]DC ^{1}H/^{15}N, signed (kHz)	1.045 ± 0.024
[a]DC ^{1}H/^{15}N, unsigned (kHz)	2.442 ± 0.041
[a]DC ^{1}HA/^{13}CA, unsigned (kHz)	1.270 ± 0.090
[b]DC ^{1}H/^{15}N, signed (kHz)	1.291 ± 0.010
[b]DC ^{1}H/^{15}N, unsigned (kHz)	1.415 ± 0.169
[b]CSA ^{15}N, non-Gly (ppm)	2.116 ± 0.038
[b]CSA ^{15}N, Gly (ppm)	2.477 ± 0.394
[c]Distances ^{13}C–^{13}C (Å)	0.046 ± 0.019
[d]Dihedral angles (°)	2.627 ± 0.078
Average pairwise RMSD for structured residues 5–69 (Å)	
Backbone heavy atoms	0.92 ± 0.36
All heavy atoms	1.78 ± 0.25
Ramachandran plot statistics from Molprobity (%)	
Residues in most favored regions	93.975 ± 2.008
Residues in outlier regions	2.947 ± 1.607
Poor rotamers	4.557 ± 2.811

[a] Measured from RA solid-state NMR experiments

[b] Measured from OS solid-state NMR experiments

[c] Measured in MAS PDSD solid-state NMR experiments

[d] Extracted from Rosetta

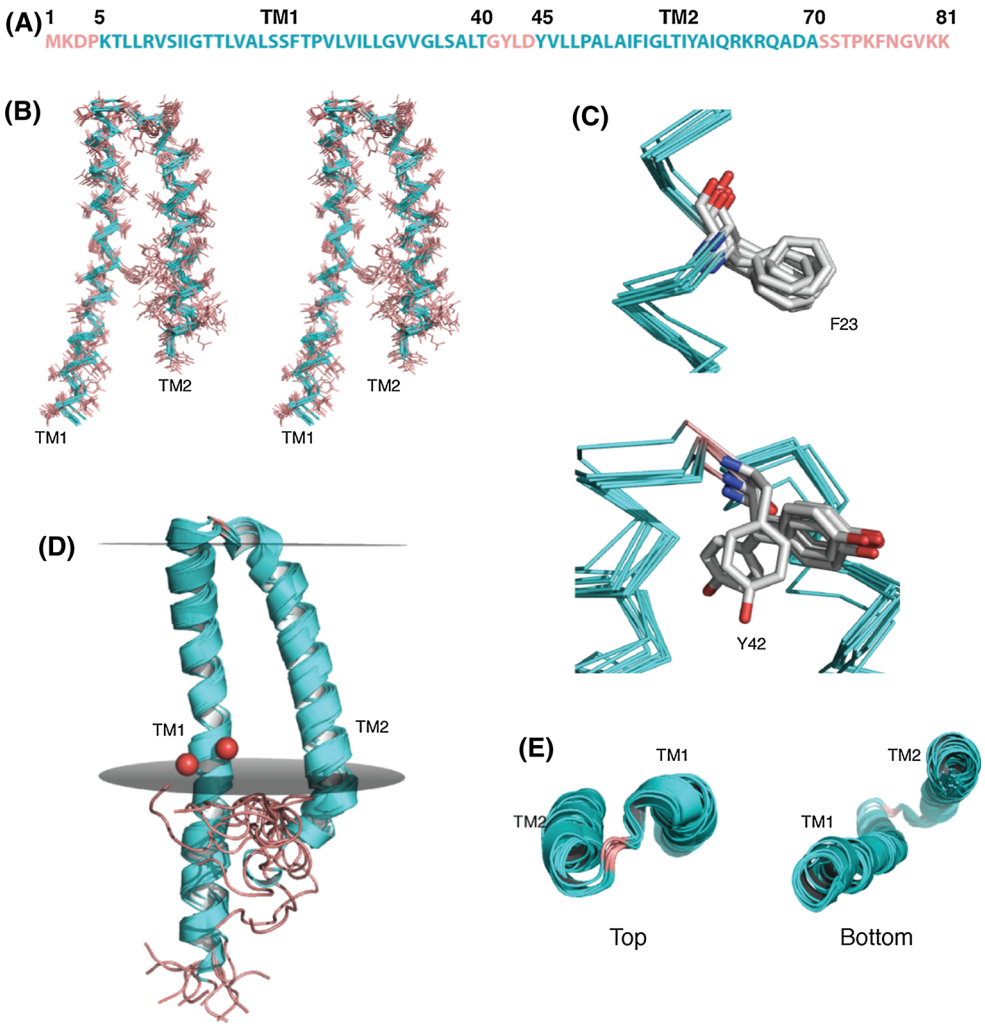

Fig. 2 Ensemble of ten lowest energy structures of MerF. **A** Primary sequence of MerF showing the identified transmembrane domains in *blue* and mobile termini and loop in *red*. **B** Stereo view of the MerF ensemble. **C** Conformations of F23 (where ^{13}C–^{13}C distance restraints were applied to side-chain atoms) and Y42 (where no distance restraints were available) in the ten lowest energy structures. **D** Ribbon representation of the MerF ensemble. The OG atoms of S21–S22 pair (C21–C22 in the wild-type protein) are shown as *red spheres*. They are near the membrane-water interface predicted based on residue hydrophobicity. The membrane-water interface is depicted as *gray discs*. **E** *Top and bottom* view showing the structured inter-helical loop between the two transmembrane domains

non-Gly residues, and $\delta_{11} = -41.0$ ppm, $\delta_{22} = -64.0$ ppm, $\delta_{33} = 105.0$ ppm, $\delta_{iso} = 105$ ppm $\beta = 20°$, and $\gamma = 0°$ for Gly residues (Oas et al. 1987; Wu et al. 1995). The torsion DB statistical torsion angle potential (Bermejo et al. 2012) was implemented with a force constant set to $k_{tDB} = 0.02$ kcal mol^{-1} rad^{-2} in the high temperature stage and ramped geometrically from 0.02 to 2 kcal mol^{-1} rad^{-2} during simulated annealing. Atomic overlap was prevented by limiting allowed repulsions to those between atoms separated by four or more covalent bonds (nbxmod = 4).

A total of 100 structures were calculated and the ten with lowest experimental energy were accepted as the representative structure ensemble of MerF. In the ensemble, residues 5–69 have a backbone RMSD of 0.92 ± 0.36 Å and all-heavy atom RMSD of 1.78 ± 0.25 Å (Table 1; Fig. 2). The final, average values of Da were estimated to be 10.32 kHz for the OS NMR restraints, and 9.90 kHz for the MAS NMR restraints, given the maximum Da value of 10.52 kHz and assuming an amide NH bond length of 1.05 Å. Structural statistics are listed in Table 1. The structure coordinates were deposited in the protein databank (PDB) with PDB ID: 2moz.

Discussion and conclusions

This manuscript describes improvements in the accuracy and precision of the structure of the mercury transporter membrane protein, MerF, under physiological conditions, as determined by solid-state NMR spectroscopy in phospholipid bilayers.

By applying a solid-state NMR INEPT experiment, we were able to obtain assignments of all mobile residues at the *N*- and *C*- termini of full-length MerF in phospholipid bilayers. Previously, we had to rely on the absence of resonances in solid-state NMR spectra, which present ambiguities in the interpretation. The experimental data in Fig. 1 show that at the N-terminal residues 1–4 and the *C*-terminus residues 70–81 are mobile on the relevant

NMR time scale of 10^{-4} s. All other residues are in stable conformations, as shown by the wide range of values of other solid-state NMR spectral parameters, on the same time scale. The ribbon representation of the ten lowest energy structures ensemble (Fig. 2d) illustrates the mobility of the terminal residues.

As shown previously for membrane proteins in lipid bilayers (Ding et al. 2013; Murray et al. 2013; Opella 2013) and for a globular crystalline protein (Wylie et al. 2011), anisotropic chemical shift frequencies provide additional structural restraints that contribute significantly to improving structural precision and accuracy. In the case of MerF, the heavy atom RMSD improved from 2.58 Å, for the structure determined without ^{15}N CSAs (PDB: 2m67), to 1.78 Å, for the structure determined here with ^{15}N CSA restraints (PDB: 2moz). Similarly, the backbone atom RMSD improved from 1.48 to 0.92 Å. Furthermore, high correlation is observed between the experimental orientation restraints and the values calculated from the final structure (Fig. S2).

These results confirm and refine the structure of MerF in phospholipid bilayers. The protein has two hydrophobic transmembrane helices and a relatively short, structured inter-helical loop. Four residues at the *N*-terminus and eleven residues at the *C*-terminus are mobile and unstructured on the relevant NMR timescales. The three-dimensional structure shows that the two pairs of Cys residues involved in binding Hg(II) are in close proximity on the cytoplasmic side of the phospholipid bilayer (Fig. 2). The details of the transport mechanism of Hg(II) from MerP to MerA are still unknown. However, the finding of vicinal pairs of Cys residues of MerF is an important first step towards synthesizing a functional model for metal ion transfer in the bacterial mercury detoxification system.

Acknowledgments This research was supported by grants from R01GM099986, P41EB002031, R01EB005161, R01GM066978, R01GM100265 and P01AI074805 from the National Institutes of Health. It utilized the BTRC for NMR Molecular Imaging of Proteins at UCSD.

References

Baldus M, Petkova A, Herzfield J, Griffin R (1998) Cross polarization in the tilted frame: assignment and spectral simplification in heteronuclear spin systems. Mol Phys 95:1197–1207

Barkay T, Miller SM, Summers AO (2003) Bacterial mercury resistance from atoms to ecosystems. FEMS Microbiol Rev 27:355–384. doi:10.1016/S0168-6445(03)00046-9

Bermejo GA, Clore GM, Schwieters CD (2012) Smooth statistical torsion angle potential derived from a large conformational database via adaptive kernel density estimation improves the quality of NMR protein structures. Protein Sci 21:1824–1836. doi:10.1002/pro.2163

Das BB, Nothnagel HJ, Lu GJ, Son WS, Tian Y, Marassi FM, Opella SJ (2012) Structure determination of a membrane protein in proteoliposomes. J Am Chem Soc 134:2047–2056. doi:10.1021/ja209464f

Ding Y, Yao Y, Marassi FM (2013) Membrane protein structure determination in membrana. Acc Chem Res 46:2182–2190. doi:10.1021/ar400041a

Hardy EH, Verel R, Meier BH (2001) Fast MAS total through-bond correlation spectroscopy. J Magn Reson 148:459–464

Kim DE, Chivian D, Baker D (2004) Protein structure prediction and analysis using the Robetta server. Nucleic Acids Res 32:W526–W531. doi:10.1093/nar/gkh468

Lu GJ, Opella SJ (2014) Resonance assignments of a membrane protein in phospholipid bilayers by combining multiple strategies of oriented sample solid-state NMR. J Biomol NMR 58:69–81. doi:10.1007/s10858-013-9806-y

Lu GJ, Tian Y, Vora N, Marassi FM, Opella SJ (2013) The structure of the mercury transporter MerF in phospholipid bilayers: a large conformational rearrangement results from N-terminal truncation. J Am Chem Soc 135:9299–9302. doi:10.1021/ja4042115

Murray DT, Das N, Cross TA (2013) Solid state NMR strategy for characterizing native membrane protein structures. Acc Chem Res 46:2172–2181. doi:10.1021/ar3003442

Oas TG, Hartzell CJ, Dahlquist W, Drobny GP (1987) The amide 15N chemical shift tensors of four peptides determined from 13C dipole-coupled chemical shift powder patterns. J Am Chem Soc 109:5962–5966

Opella SJ (2013) Structure determination of membrane proteins in their native phospholipid bilayer environment by rotationally aligned solid-state NMR spectroscopy. Acc Chem Res 46:2145–2153. doi:10.1021/ar400067z

Schiering N, Kabsch W, Moore MJ, Distefano MD, Walsh CT, Pai EF (1991) Structure of the detoxification catalyst mercuric ion reductase from Bacillus sp. strain RC607. Nature 352:168–172. doi:10.1038/352168a0

Schwieters CD, Clore GM (2001) Internal coordinates for molecular dynamics and minimization in structure determination and refinement. J Magn Reson 152:288–302

Schwieters CD, Kuszewski JJ, Tjandra N, Clore GM (2003) The Xplor-NIH NMR molecular structure determination package. J Magn Reson 160:65–73. doi:10.1016/S1090-7807(02)00014-9

Steele RA, Opella SJ (1997) Structures of the reduced and mercury-bound forms of MerP, the periplasmic protein from the bacterial mercury detoxification system. Biochemistry 36:6885–6895. doi:10.1021/bi9631632

Tian Y, Schwieters CD, Opella SJ, Marassi FM (2012) AssignFit: a program for simultaneous assignment and structure refinement from solid-state NMR spectra. J Magn Reson 214:42–50. doi:10.1016/j.jmr.2011.10.002

Wilson JR, Leang C, Morby AP, Hobman JL, Brown NL (2000) MerF is a mercury transport protein: different structures but a common mechanism for mercuric ion transporters? FEBS Lett 472:78–82. doi:10.1016/S0014-5793(00)01430-7

Wu C, Ramamoorthy A, Gierasch LM, Opella SJ (1995) Simultaneous characterization of the amide 1H chemical shift, 1H-15N dipolar, and 15N chemical shift interaction tensors in a peptide bond by 3-dimensional solid-state NMR spectroscopy. J Am Chem Soc 117:6148–6149

Wylie BJ, Sperling LJ, Nieuwkoop AJ, Franks WT, Oldfield E, Rienstra CM (2011) Ultrahigh resolution protein structures using NMR chemical shift tensors. Proc Natl Acad Sci USA 108:16974–16979. doi:10.1073/pnas.1103728108

Yarov-Yarovoy V, Schonbrun J, Baker D (2006) Multipass membrane protein structure prediction using Rosetta. Proteins 62:1010–1025. doi:10.1002/prot.20817